Article

Not peer-reviewed version

Study on the Influences of Idler Materials on Rolling Electrical Contact Performance

Haihong Wu , Zhiyuan Qian , Chuankun Qu , Lei Zhang , Huiqun Liu , Xiao Kang *

Posted Date: 25 September 2024

doi: 10.20944/preprints202409.2033.v1

Keywords: flexible ring; Idler; electrical contact; material transfer; wear

Preprints.org (www.preprints.org) | NOT PEER-REVIEWED | Posted: 25 September 2024 doi:10.20944/preprints202409.2033.v1

Article

Study on the Influences of Idler Materials on Rolling Electrical Contact Performance

Haihong Wu [1,2], Zhiyuan Qian [3], Chuankun Qu [3], Lei Zhang [4], Huiqun Liu [1] and Xiao Kang [4,*]

1 School of Materials Science and Engineering, Central South University, Changsha, Hunan, 410083
2 CSSC Jiangxi Jiujiang Marine Equipment Co., Ltd., Jiujiang, Jiangxi, 332008
3 National Key Laboratory of Aerospace Mechanism， Aerospace System Engineering Shanghai, Shanghai, 201108, China
4 State Key Laboratory of Powder Metallurgy, Central South University, Changsha 410083, China
* Correspondence: kangxiao0601@csu.edu.cn

Abstract: The parallel connection of multiple flexible rings in raceways can significantly improve the electrical conductivity of rolling conductive devices. Multiple flexible rings are generally separated by idlers to form ring-idler rolling pairs. In the present work, alumina (Al_2O_3), polytetrafluoroethylene (PTFE), polyether ether ketone (PEEK), and polyimide (PI) were used as idler materials. Rolling tests for four types of ring-idler contact pairs were carried out in the air at a rotating speed of 10 rpm and a current of 60 A. It was noticed that the voltage drop was the lowest when Al_2O_3 was incorporated as the idler material. The energy spectrum analysis indicated material transfer between the organic idlers and the flexible ring. Especially on the flexible ring surface, the transferred organic thin film covered the gold-plated layer of the flexible ring and affected the electrical contact of the flexible ring. The transfer of Al_2O_3 was not obvious, and the mass fraction of Au on the flexible ring surface after the rolling test was 93.1%. The above results could help in selecting the best idler material for high-power conductive rotary joints.

Keywords: flexible ring; Idler; electrical contact; material transfer; wear

1. Introduction

Conductive roller rings are used to realize electrical contacts in rotating equipment. With the advancement of technology, the material, design, and application fields of conductive roller rings are evolving.

1.1. Research Background

Rolling conductive devices are a new type of rotating electrical transmission equipment [1,2], and they have a longer life, higher power, better reliability, lower frictional torque, and lower noise in comparison to traditional slip rings [1,3]. To improve the electrical conductivity of rolling conductive devices, a parallel conduction system of multiple flexible rings is generally adopted and multiple flexible rings are separated by insulated idler wheels. The general structure of a rolling conductive device is presented in Figure 1.

Preprints.org (www.preprints.org) | NOT PEER-REVIEWED | Posted: 25 September 2024 doi:10.20944/preprints202409.2033.v1

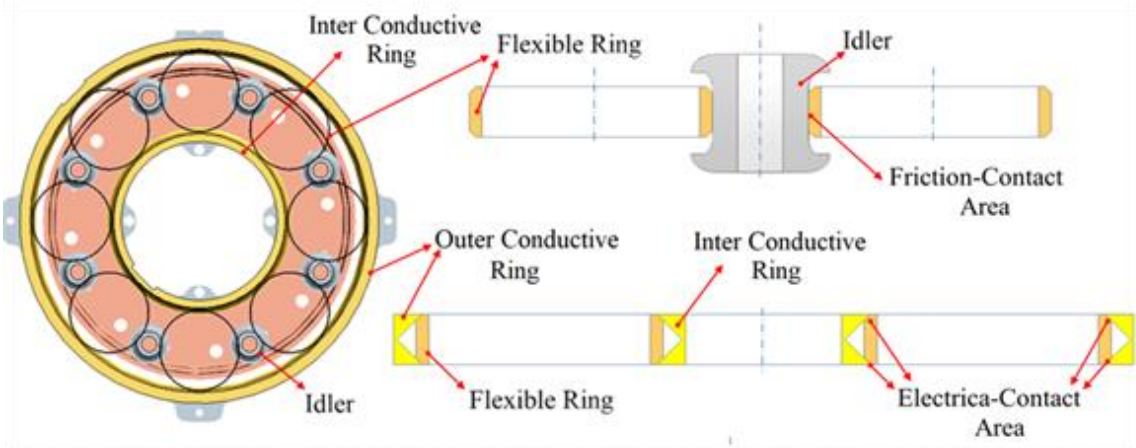

Figure 1. Structure of a single layer of a rolling conductive device.

In a rolling conductive device, the side walls of the flexible ring possess two different functional zones: (i) the frictional contact area between idlers and the flexible ring and (ii) the electrical contact area between the raceway and the flexible ring. Due to the close proximity of these two areas, products from the frictional contact area may interfere with the conductive area. When frictional products spread to the conductive area, the conductive rolling contact between the flexible ring and the raceway is damaged by the insulation material, resulting in a fluctuation in resistance [4,5]. Idlers must be insulated to avoid current crosstalk between conductive rings; hence, self-lubricating organic materials and ceramics are generally preferred.

Cai Y et al. [6] used a variety of acids, such as alkyl sulfuric acid, alkyl phosphonic acid, and alkyl boric acid, to prepare a new type of esterified cellulose nanocrystals and reported that these heterogeneous elements formed a friction transfer film in the presence of frictional heat generated from their reaction with the metal surface, resulting in a reduction in friction and wear resistance.

Yan Z et al. [7] stated that silver (Ag) nanocrystals dispersed in tungsten disulfide (WS) crystals played an important role in binding and enhancing the microstructure of the transfer film and revealed the lubrication mechanism of the WS-AG film by explaining the transfer behavior of the WS-AG film in the sliding contact zone.

Raut A et al. [8] studied the effects of reinforced fillers on the tribological properties of polytetrafluoroethylene (PTFE) composites and pointed out that in comparison to carbon black, bronze, and graphite fillers, aromatic thermosetting copolyester (ATSP)-reinforced PTFE exhibited better wear resistance and lower friction. The wear performance of PTFE-ATSP blends was improved due to their high mechanical strength and their ability to form a fluorine-rich transfer film on the 440C stainless steel interface. Hence, PTFE-ATSP blends provide an effective solution for non-lubricated engineering applications aiming at sustainable environments [9,10].

Lv X et al. [11] investigated the tribological behavior of polyether ether ketone (PEEK)-based composites with an alternating lamellar structure fabricated by the melt deposition method and asserted that the addition of solid lubricants, such as graphite, polytetrafluoroethylene, molybdenum disulfide, and boron nitride improved the friction and wear properties of the fiber-reinforced polymer composites by reducing adhesion at the friction interface and promoting the formation of a transfer membrane.

Transfer films play significant roles in tribological performance, and their characteristics are generally temperature-dependent. Longxiao Z et al. [12] found that the PTFE content in the transfer film increased as the temperature decreased. However, the friction coefficient (COF) did not follow a linear trend with temperature, and the minimum and maximum values were detected at 110ºC and −180ºC, respectively. The ATSP (aromatic thermosetting copolyester) coating manifested superior performance with lower friction and unnoticeable wear at all temperatures, whereas the PEEK coating experienced the maximum wear at 25ºC followed by at 110ºC and −180ºC. It was also observed that the larger the maximum thickness of the transfer film, the lower the wear rate, and similarly, the higher the coverage of the transfer film, the lower the wear rate. It is proved that tribo-physicochemical interactions play a crucial role in the formation of tough and wear-resistant polymer–metal interfaces [13,14].

The COF of PEEK composites in a dry and vacuum environment is lower than that in the air [15–17]. The tribological behavior of PEEK composites is determined by the wear behavior and formation mechanism of the transfer film and is generally influenced by the filler content. Theiler et al. [18,19] noted that although the composite synthesized with MoS_2 had high wear resistance under cryogenic vacuum conditions, a transfer film was formed as the contact load increased.

However, very little amount of research has been conducted on the rolling friction and wear of idlers and flexible rings. To improve the electrical contact reliability of rolling conductive devices, significant research on the selection and evaluation of idler materials should be urgently performed.

In the present work, alumina (Al_2O_3), PTFE, PEEK, and polyimide (PI) were prepared into idlers and installed into rolling products. The wear properties of different rolling pairs and the electrical contact properties of rolling conductive devices were studied. The results obtained from this experiment might be helpful for the selection of idler materials and the failure analysis of high-power conductive rotary joints.

2. Experimental Section

2.1. Idler-Flexible Ring Pairs

The idler wheels separated multiple flexible rings and formed rolling friction pairs with the flexible rings (Figure 2). The width, outer circle diameter, and wall thickness of the flexible rings were 5 mm, 38.5 mm, and 0.3 mm, respectively. The raw material of the flexible rings was beryllium bronze C17200, and a composite coating of Cu/Ni/Au was coated on them. The thicknesses of the Cu, Ni, and Au layers were 1.8–2.5 μm, 4–7 μm, and 4–7 μm, respectively. The hardness and roughness (Ra) of the coating surface were 90–100 Hv and 0.4 μm, respectively.

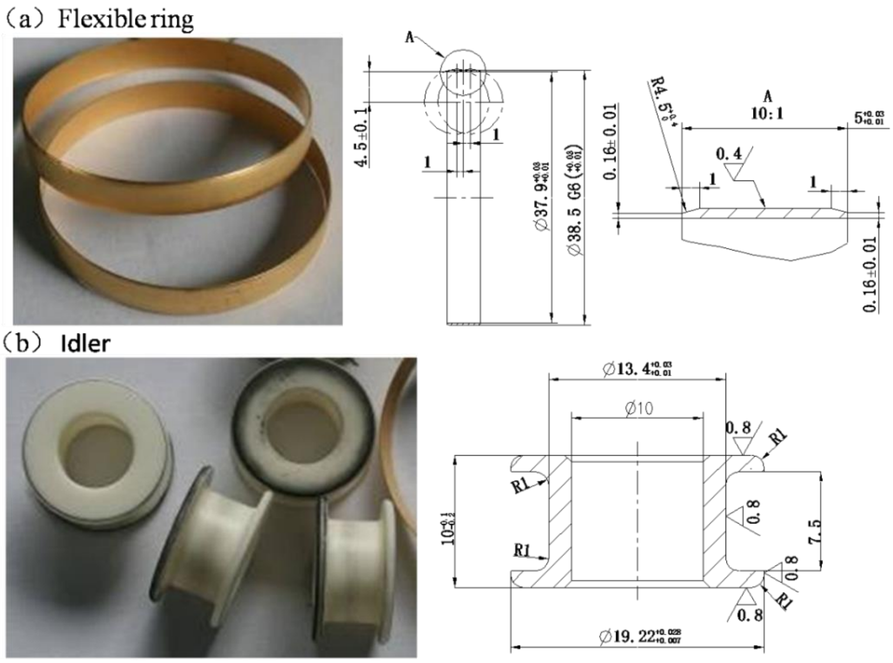

Figure 2. Idler-flexible ring friction pairs (a) Flexible rings after the test and (b) Shape of the idlers after the test.

The idler wheels possessed a hollow cap structure. The outer circle diameter of the idler wheels corresponding to the contact area of the flexible rings was 19.22 mm, and their hollow diameter was 10 mm. The basic parameters of different types of idler wheels are listed in Table 1. Al_2O_3 is a wear-

 doi:10.20944/preprints202409.2033.v

resistant insulating ceramic material, whereas PTFE, PEEK, and PI are self-lubricating insulating polymers.

Table 1. Basic performance parameters of idler wheels.

Idler material	Parameters		
	Roughness (μm)	Hardness (Hv)	Molecular formula
PTFE	about0.8	5	$(C_2F_4)_n$
PI	about0.8	108	$(C_{35}H_{28}N_2O_7)_n$
PEEK	about0.8	211	$(C_{19}H_{12}O_3)_n$
Al_2O_3	about0.8	920	Al_2O_3

2.2. Test Equipment and Methods

To make the experiment closer to engineering applications, all tests were carried out on assembled conductive joints. In Figure 3, the single-layered structure consists of eight flexible rings and eight idlers. The adjacent two layers form a conductive circuit, and the same idlers are used in the same circuit. The two conductive circuits are composed of four layers. The contact force between the flexible ring and the raceway was 0.6 N, and that between the flexible ring and the idler gears was also 0.6 N.

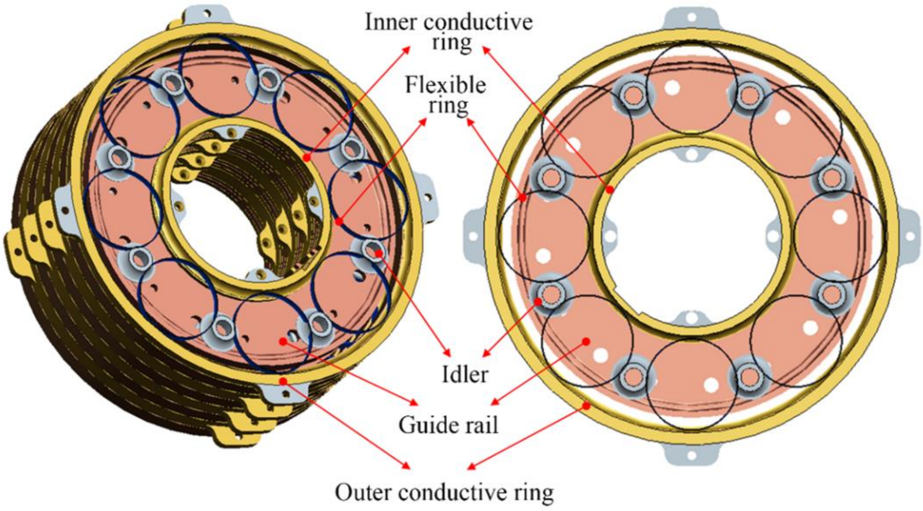

Figure 3. Structure of a rolling device consisted of four layers of conductive rings.

The voltage drop test method was adopted to evaluate the interference of the idler gears on the conductivity of the rolling device, and its working principle is illustrated in Figure 4. First, the four layers of conductive rings were connected in series to form a conductive path. The constant voltage source supplied power to wire A, and current flowed through each conductive layer through wire B and returned to the power source. The same type of idlers were used in the first and second layers of conductive rings. Test lines 1 and 2 were connected to the outer ring, and the voltage drop (V_1) was measured. The value of V_2 was also obtained using the same method.

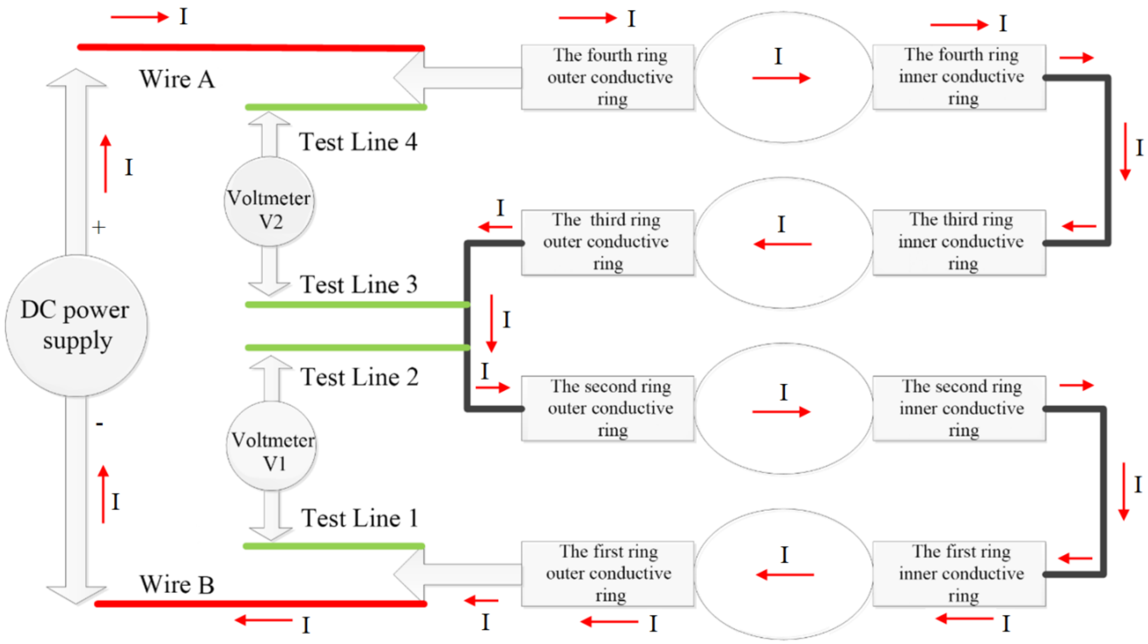

Figure 4. Voltage drop test method.

The assembled rolling device was placed on a driving mechanism, and the driving shaft was connected to the inner ring of the device. During the experiment, the inner ring rotated continuously, whereas the outer ring remained stationary. Therefore, the test line in Figure 4 remained untangled. The test was executed at normal temperature and pressure. The rotating speed, current, and total rotating cycles were 10 rpm, 60 A, and 90,000 revolutions, respectively.

2.3. Surface Characterization

To analyze the wear and material transfer mechanisms of the idler-flexible ring pairs, the microstructure of the contact surface was observed by an optical microscope (OM; VR-5000, Keene, Japan) and a scanning electron microscope (SEM; Tescan Mira4, Czech Republic) equipped with an energy-dispersive spectrometer (EDS; Xplore30. Aztec one, USA).

3. Results and Analysis

3.1. Influence of Idler Materials on the Electrical Contact Properties of Rolling Rings

When the test current was constant, the voltage drop was determined by the contact resistance. It was found that the larger the voltage drop, the worse the electrical contact performance. Under a constant current of 60 A, the initial voltage drop of the four pairs of flexible rings was about 0.15 V, and their initial electrical contact states were the same. When the rolling ring started to rotate, the change in voltage drop for each circuit was recorded (Figure 5). The voltage drop for Al_2O_3 increased after 25,000 cycles; however, the change was very small. The voltage drop for Al_2O_3 at 30,000 cycles rapidly increased to 0.21 V and subsequently slowly increased to 0.23 V. The voltage drop for PEEK changed sharply and increased significantly after 47,000 cycles and finally reached 0.37 V after 90,000 cycles. The voltage drop for PTFE slowly increased before 82,000 cycles and suddenly increased in the subsequent process. The voltage drop for PI increased very slowly before 85,000 cycles, and the value reached 0.27 V after 90,000 cycles. Hence, it is noticeable that the electrical contact performance deteriorated earlier when Al_2O_3 and PEEK were used as idlers, and the degree of electrical contact deterioration by Al_2O_3 was lower. When PTFE and PI were used as idlers, the electrical contact properties remained unchanged for a long time; however, the final negative effects were very prominent. Therefore, Al_2O_3 was more suitable as the idler material.

Preprints.org (www.preprints.org) | NOT PEER-REVIEWED | Posted: 25 September 2024 doi:10.20944/preprints202409.2033.v1

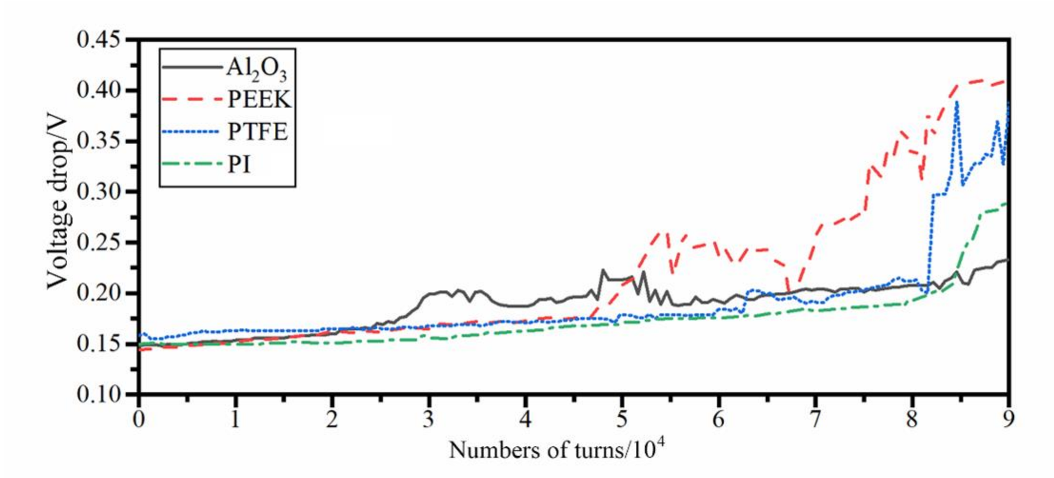

Figure 5. Effects of different idler materials on voltage drop in rolling rings.

3.2. Wear and Material Transfer of Idler-Flexible Ring Pairs

The electrical contact properties of different idler-flexible ring pairs after rolling for 90,000 cycles deteriorated to varying degrees, indicating that the Au coating layer was damaged or covered with non-conductive materials. To reveal the mechanism of electrical conductivity deterioration, the contact surfaces of idler-flexible ring pairs were observed by OM. Some processing traces were observed on the original flexible ring surface (Figure 6a). After rolling with PEEK and PTFE, some black materials were detected on the flexible ring surface (Figure 6b and 6c). After rolling with PI, the metallic luster and black spots were evenly distributed on the flexible ring surface (Figure 6d). After rolling with Al_2O_3, the color of the flexible ring surface was similar to the original state; however, the number of scratches increased (Figure 6d).

The microstructures of different idler surfaces were also observed by OM. The surfaces of PEEK and PTFE contained a huge amount of metallic debris; however, the amount of metallic debris on the PI surface was small. The surface of Al_2O_3 experienced no obvious change, implying that material transfer occurred between the organic idlers and the flexible rings.

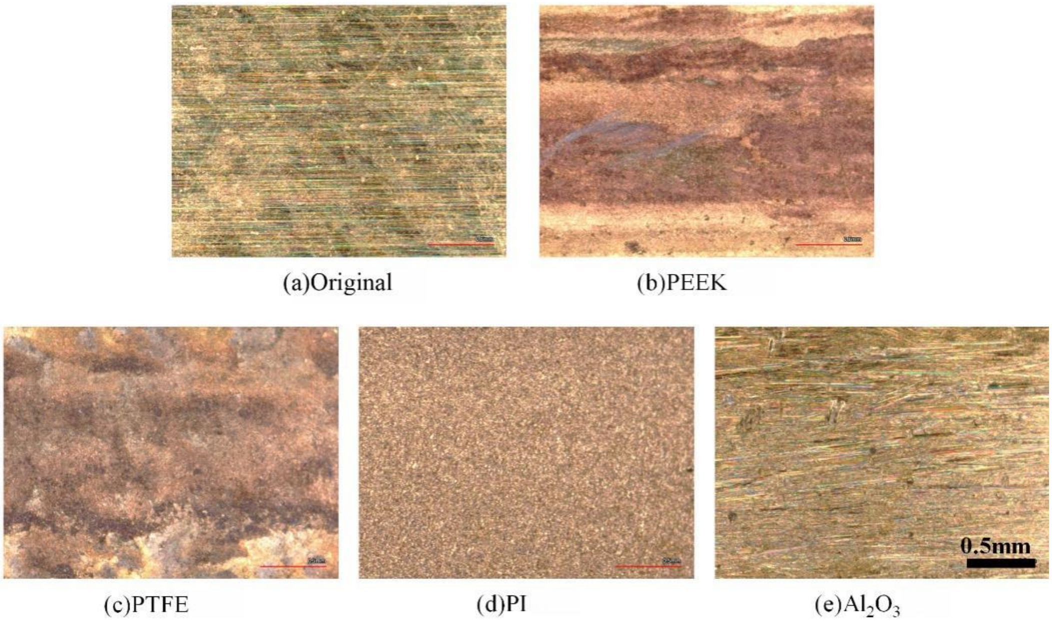

Figure 6. Optical images of the surfaces of the flexible rings after rolling with different idlers.

Preprints.org (www.preprints.org) | NOT PEER-REVIEWED | Posted: 25 September 2024 doi:10.20944/preprints202409.2033.v1

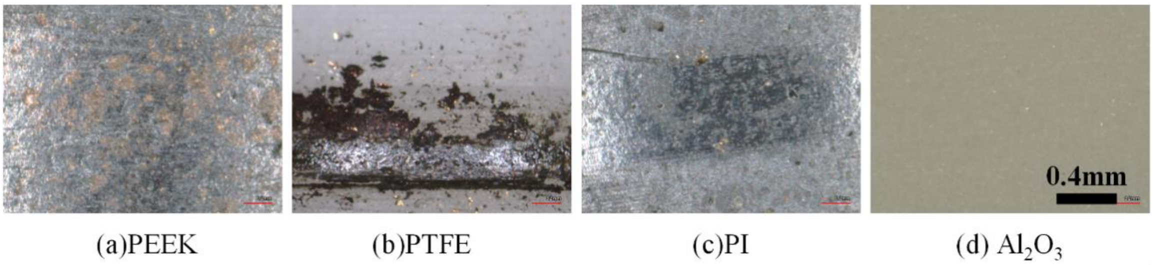

Figure 7. Optical images of different idler surfaces after rolling.

The surfaces of the idler-flexible ring pairs after rolling were further observed by SEM. A large amount of flakes with a small number of black patches appeared on the PEEK surface (Figure 8a). A large amount of debris was detected on the PTFE surface, and some black patches existed on the flexible ring surface (Figure 8b). The surface of the PI idlers was slightly worn, and the flexible ring surface was smeared with small black spots (Figure 8c). Prominent scratches generated from abrasive wear by Al_2O_3 were found on the flexible ring surface (Figure 8d), and some white flakes were observed on the Al_2O_3 surface. These results further confirm that material transfer occurred between the idlers and the flexible rings, and the wear mechanism was dominated by adhesion and abrasive wear. The damage of the PI idler-flexible ring and Al_2O_3 idler-flexible ring pairs was relatively low, and this finding is consistent with the electrical contact results in Figure 5.

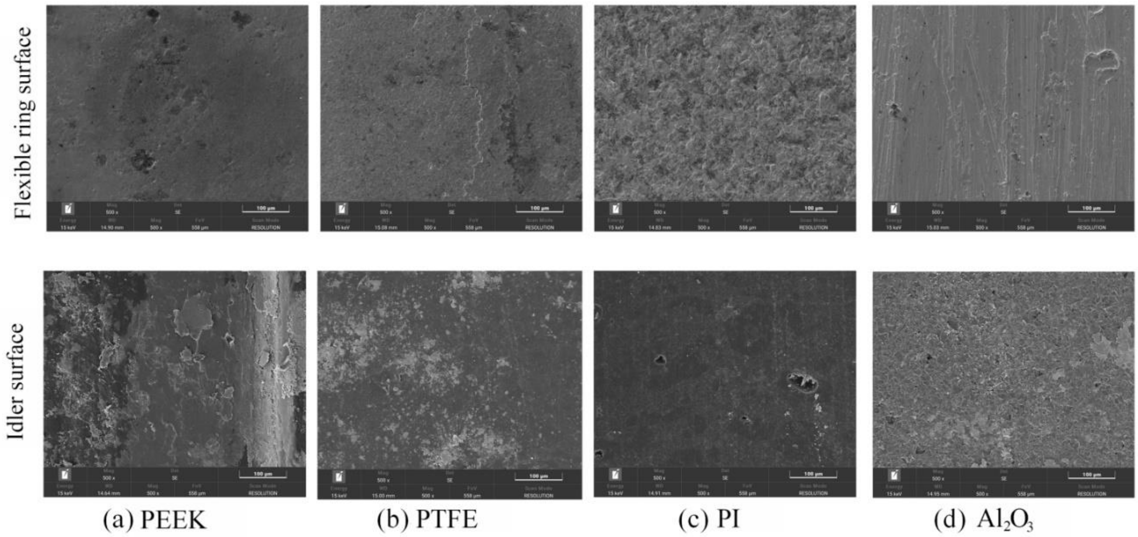

Figure 8. SEM images of the surfaces of different idler-flexible ring pairs after rolling.

To analyze the main reasons for the deterioration of electrical contact properties, the energy spectrum in the scanning model was used to evaluate the material transfer process on the worn surface. For the PEEK-flexible ring pair, some small black patches were scattered on the flexible ring surface (Figure 9; the white area contained C and O, which were derived from PEEK). The main components of large white flakes on the PEEK idlers were Au, Ni, and Cu, indicating that the Au coating on the flexible ring surface was transferred to the idler surface. The Au mass fraction on the flexible ring surface after rolling was 82.7%. The wear of the Au coating and the coverage of organic matter both reduced the Au content on the flexible ring surface and caused a decrease in electrical conductivity.

Preprints.org (www.preprints.org) | NOT PEER-REVIEWED | Posted: 25 September 2024 doi:10.20944/preprints202409.2033.v1

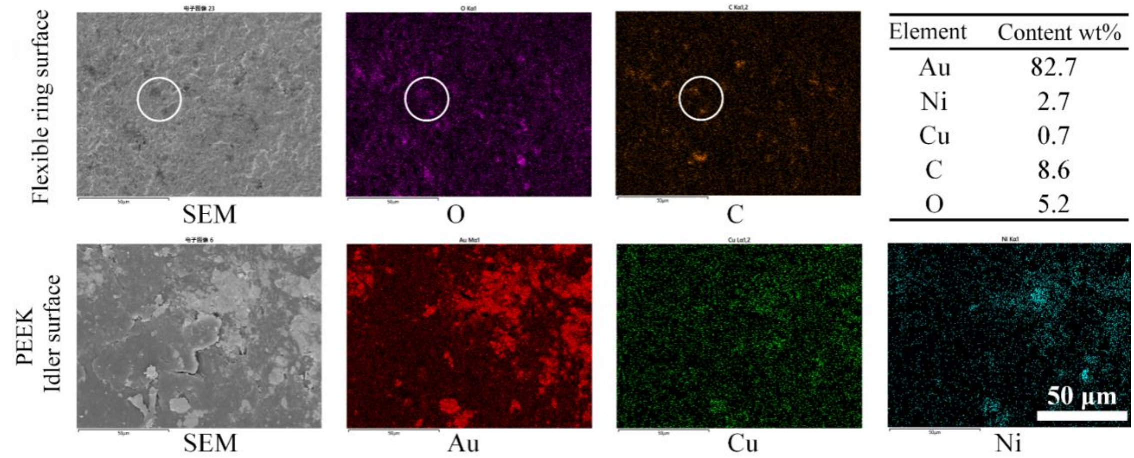

Figure 9. EDS results for the PEEK idler-flexible ring pair.

The phenomenon of material transfer was also observed in the PTFE idler-flexible ring pair (Figure 10; the carbon content in the white area was very high). As PTFE does not contain oxygen, the high oxygen content in the white area could be attributed to the oxidation of Cu or Ni. A sheet-like transfer material was detected on the PTFE surface, and the main components of this material were Au, Ni, and Cu (the signal of Cu was very prominent). The flexible ring surface was severely worn, and the Au coating was seriously damaged. The mass fractions of Au and C on the flexible ring surface were 53.5% and 15.8%, respectively, after rolling.

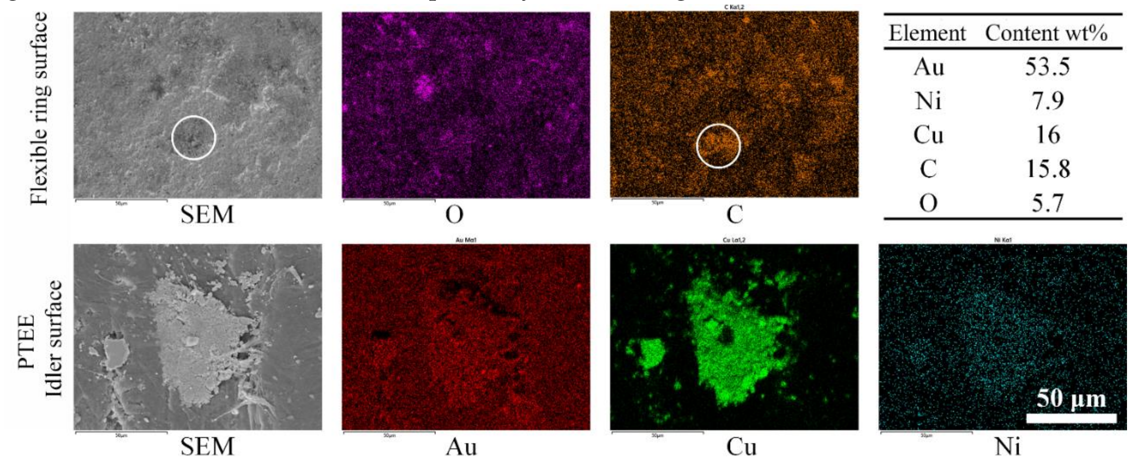

Figure 10. EDS results for the PTFE idler-flexible ring pair.

Some black spots were observed on the PI idler-flexible ring contact surface (Figure 11; C and O signals, which were derived from PI, in the white areas were prominent). The Cu content on the entire surface was zero, indicating that the Au film was not damaged and still covered the Cu substrate. Fine white products of Au were detected on the PI idler surface. After the rolling test, the mass fractions of Au and C on the flexible ring surface were 79.9% and 15.5%, respectively, confirming that material transfer occurred between the flexible rings and the PI idlers.

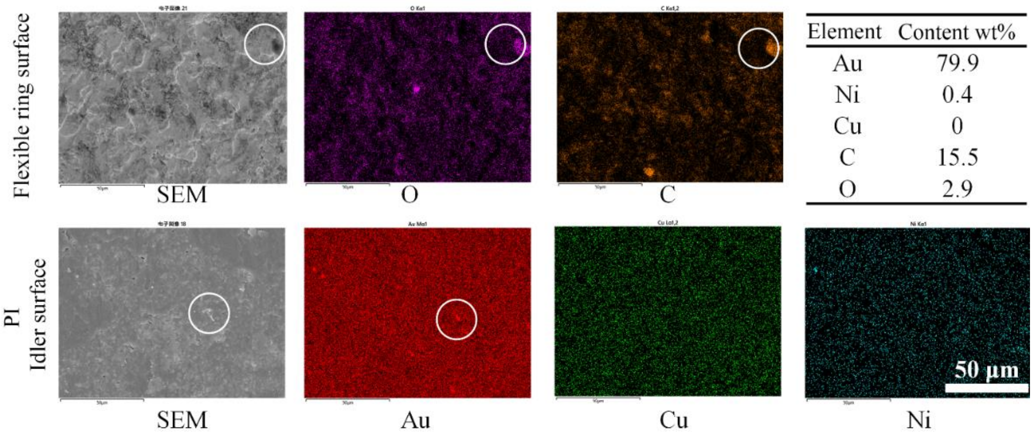

Figure 11. EDS results for the PI idler-flexible ring pair.

A large number of scratches with a small amount of particles were found on the Al_2O_3 idler-flexible ring contact surface (Figure 12; the white areas contained Al and O, which came from the Al_2O_3 idlers). Some fine wear products of Cu were observed on the idler surface. The mass fraction of Au on the flexible ring surface after rolling was 93.1%, implying that material transfer between the flexible rings and the Al_2O_3 idler gears was not obvious. The complete Au film on the flexible ring surface ensured good electrical conductivity.

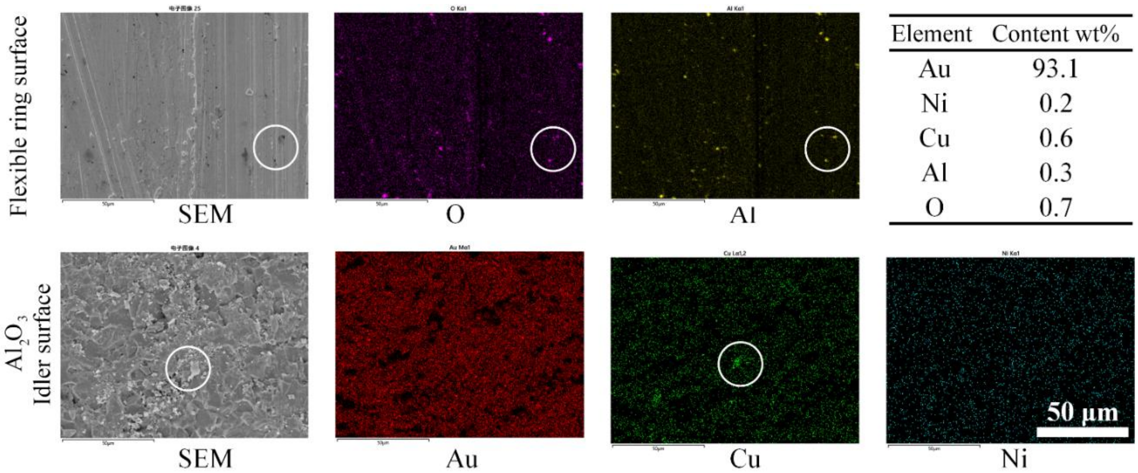

Figure 12. EDS results for the Al_2O_3 idler-flexible ring pair.

During the rolling test, changes in the electrical contact performances of different idler-flexible ring pairs were observed. The friction and wear morphologies of the electrical contact area of the flexible rings were analyzed by SEM. Non-metallic transfer film layers were found in the friction area between the idlers and the flexible rings (Figure 13).

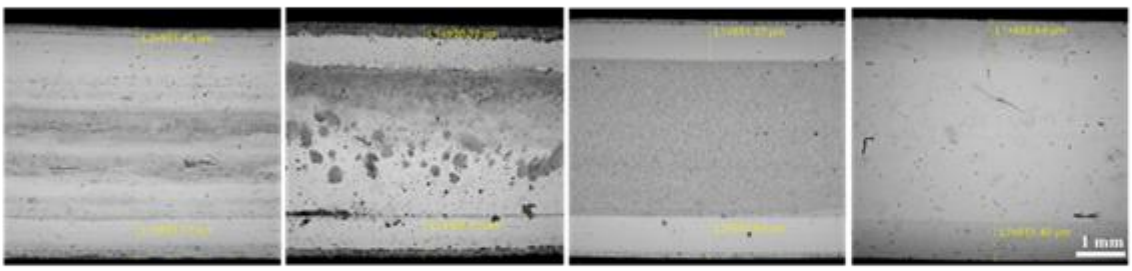

(a) PEEK idler-flexible ring (b) PTFE idler-flexible ring (c) PI idler-flexible ring (d) Al_2O_3 idler-flexible ring

Preprints.org (www.preprints.org) | NOT PEER-REVIEWED | Posted: 25 September 2024 doi:10.20944/preprints202409.2033.v1

Figure 13. SEM images of the friction and wear morphologies in the contact area of different idler-flexible ring pairs after rolling.

A large number of block-like black areas with C, O, and Au mass fractions of 56%, 18.2%, and 21.9%, respectively, appeared in the electrical contact area of the PEEK idler-flexible ring pair (Figure 14).

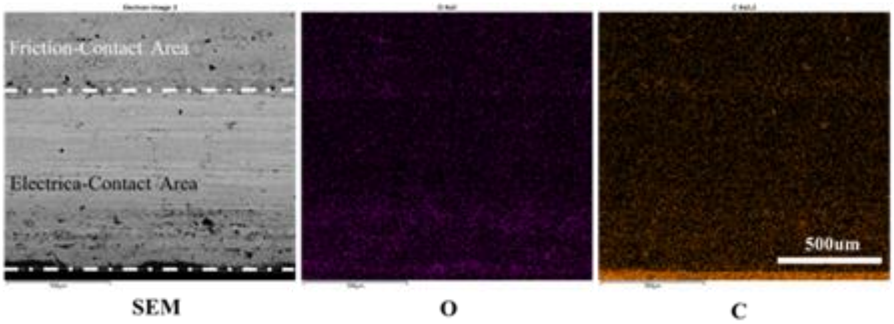

Element	Content wt%
Au	21.9
Ni	3.2
Cu	0.6
C	56.0
O	18.2

Figure 14. EDS results for the electrical contact and friction contact surfaces of the PEEK idler-flexible ring pair.

A large number of black spots with C, O, and Au mass fractions of 58.9%, 11.6%, and 22.9%, respectively, were detected in the electrical contact area of the PTFE idler-flexible ring pair (Figure 15).

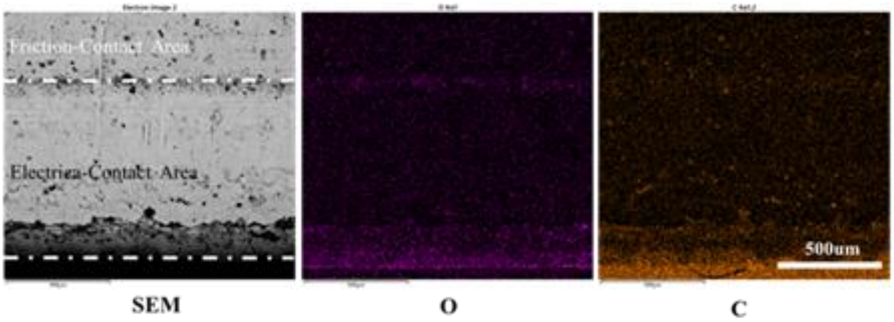

Element	Content wt%
Au	22.9
Ni	2.2
Cu	4.5
C	58.9
O	11.6

Figure 15. EDS results for the electrical contact and friction contact surfaces of the PTFE idler-flexible ring pair.

It is noticeable from Figure 16 that some black spots with C, O, and Au mass fractions of 63.7%, 9.1%, and 25%, respectively, existed on the contact surface of the PI idler-flexible ring pair.

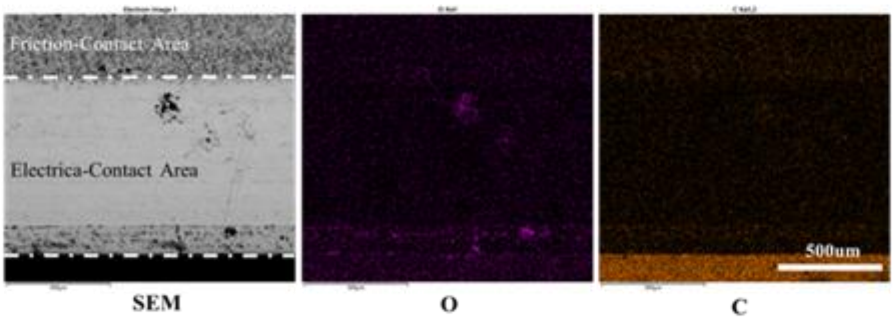

Element	Content wt%
Au	25.0
Ni	1.9
Cu	0.4
C	63.7
O	9.1

Figure 16. EDS results for the electrical contact and friction contact surfaces of the PI idler-flexible ring pair.

Figure 17 reveals the presence of a small amount of scratches with Au, Al, and O mass fractions of 87.3%, 6.9%, and 5.1%, respectively, on the electrical contact surface of the Al_2O_3 idler-flexible ring pair.

 doi:10.20944/preprints202409.2033.v1

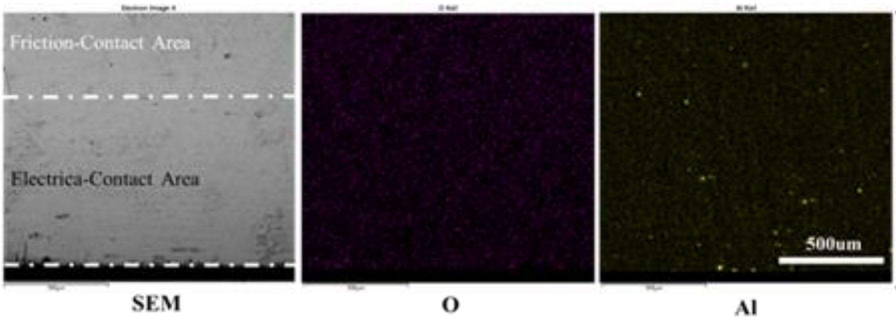

Element	Content wt%
Au	87.3
Ni	0.7
Cu	0
Al	6.9
O	5.1

Figure 17. EDS results for the electrical contact and friction contact surfaces of the Al_2O_3 idler-flexible ring pair.

It can be inferred from the above results that the electrical contact performance of the flexible rings was closely related to material transfer between idler-flexible ring pairs. After the polymer (PI, PTFE, or PEEK) was transferred to the flexible ring surface, it spread to the electrical contact area through diffusion and plastic flow. The polymer transfer film increased the film resistance at the electrical contact interface and consequently reduced the electrical contact performance of the flexible rings. The transfer film was discontinuous and uneven, resulting in fluctuations of contact resistance. PTFE had the lowest hardness and was more prone to material transfer; thus, the PTFE idler-flexible ring pair exhibited the worst performance. Al_2O_3 had the highest hardness and was difficult to transfer. Moreover, the Au coating on the flexible ring surface was not covered; hence, the Al_2O_3-flexible ring pair yielded the best electrical contact performance.

The polymer idlers had two impacts on rolling ring products—they caused a self-lubricating effect to reduce the wear of the Au layer and also induced material transfer. When the transfer film spread to the electrical contact area, the average value of voltage drop increased, leading to a deterioration in the electrical conductivity of the rolling ring. However, in the case of the Al_2O_3-flexible ring pair, the formation of a transfer film was hindered.

4. Conclusions

Four types of idler gears—Al_2O_3, PTFE, PEEK, and PI—are used to form rolling pairs with flexible rings, and they were assembled into rolling ring products for electrical conductivity tests. Voltage drops were recorded in real-time during rolling to evaluate the degradation of the electrical contact performance of the rolling pairs. The wear and material transfer rates of the rolling pairs were evaluated, and the degradation mechanism of the electrical contact performance of the rolling ring was analyzed. Material transfer between the organic idlers and the flexible ring was detected by SEM and EDS, and organic transfer films were found to be harmful to electrical contacts due to their expansion to conductive regions. The transfer of Al_2O_3 to the flexible ring surface was not obvious. The Au mass fraction on the flexible ring surface was 93.1%, resulting in the best electrical contact performance among the four rolling pairs. These results could provide important references for the selection of idler materials for rolling ring products.

Acknowledgments: The authors thank the China Aerospace Science and Technology Corporation for the financial support under the Open Project Fund of the National Key Laboratory of the Aerospace and Space Agency.

References

1. P.E. Jacobson, Rolling electrical transfer coupling improvements, EP, 2003.
2. C. Junxing, R. Mingzhe, Y. Fei, W. Yi, S. Hao, Y. Yun, Numerical research on the electrical contact model and thermal analysis of the Roll-Ring, 2013 2nd International Conference on Electric Power Equipment - Switching Technology (ICEPE-ST), 2013, pp. 1-4.

Preprints.org (www.preprints.org) | NOT PEER-REVIEWED | Posted: 25 September 2024 doi:10.20944/preprints202409.2033.v1

3. X. Hou, L. Wang, Q. Li, J. Wang, J. Liu, Review of Key Technologies for High-Voltage and High-Power Transmission in Space Solar Power Station, Transactions of China Electrotechnical Society 33(14) (2018) 3385-3395.
4. Y. Sun, C. Song, Z. Liu, J. Li, Y. Sun, B. Shangguan, Y. Zhang, Effect of relative humidity on the tribological/conductive properties of Cu/Cu rolling contact pairs, Wear 436-437 (2019) 203023.
5. T. Chen, C. Song, Y. Zhang, K. Niu, Z. Liu, L. Wang, C. Sun, M. Li, Y. Zhang, Current-carrying contact character and wear behavior of an elastic ring at different rolling speeds, Engineering Failure Analysis 131 (2022) 105825.
6. Cai Y, Meng Y, Cheng Y , et al. Alkylboronic acid esterified cellulose nanocrystal by an improved green method as an efficient lubricant nanoadditive for friction and wear reduction[J].Chemical Engineering Journal,2024,496153912-153912.
7. Yan Z, Liu J ,Shi X , et al. Tribological properties and transfer behaviors of WS2-Ag nanocomposite films with structure evolution for aerospace application[J].Applied Surface Science,2024,674160928-160928.
8. Raut A, Nunez E E ,Sellers R , et al. The effect of reinforcing fillers on the tribological performance of PTFE composites for a sustainable environment[J].Wear,2024,556-557205524-205524.
9. Kian B, Vasilis T, Ahmad A , et al. Polymer transfer film formation from cryogenic to elevated temperatures[J].Friction,2024,12(9):2018-2032.
10. Yan C, Zhang Y, Zeng Q, et al. Comparative investigation on the tribocorrosion resistance of Ti6Al4V and 60NiTi alloys inimulated seawater environment[J].Wear,2024,550-551205423-..
11. Lv X, Pei X, Yang S , et al. Tribological behavior of PEEK based composites with alternating layered structure fabricated via fused deposition modeling[J].Tribology International,2024,199109953-109953.
12. Longxiao Z, Ting X, Kun C, et al. Quantitative characterization of the transfer film morphology of SiO2/PTFE composite[J].Wear,2021,484-485
13. Zhang K, Lin Z, Chen J, et al. An ingenious synergistic solid lubricant of copper and graphite for exceptional wear resistance of the SCF/PTFE/PEEK composite[J].Tribology International,2024,195109583.
14. Ren B, Gao L ,BotaoXie, et al. Tribological properties and anti-wear mechanism of ZnO@graphene core-shell nanoparticles as lubricant additives[J].Tribology International,2020,144106114-106114.
15. Oyamada, T., Ono, M., Miura, H., & Kuwano, T. (2013). Effect of Gas Environment on Friction Behavior and Tribofilm Formation of PEEK/Carbon Fiber Composite. Tribology Transactions, 56(4), 607–614.
16. McCook N, Hamilton M, Burris D , et al. Tribological results of PEEK nanocomposites in dry sliding against 440C in various gas environments[J].Wear,2007,262(1-2):1511-1515.
17. Theiler G, Gradt T. Environmental effects on the sliding behaviour of PEEK composites[J].Wear,2016,368-369278-286.
18. Nikonovich M, Ramalho A, Emami N .Effect of cryogenic aging and test-environment on the tribological and mechanical properties of PEEK composites[J].Tribology International,2024,194109554-.
19. Theiler G, Gradt T. Friction and wear of PEEK composites in vacuum environment[J].Wear,2010,269(3):278-284.